

A resolution criterion based on characteristic time-scales for MHD simulations of molecular clouds

Guido Granda-Muñoz,^{1*} Enrique Vázquez-Semadeni,^{1†} Gilberto C. Gómez,^{1‡} and Manuel Zamora-Avilés²

¹*Instituto de Radioastronomía y Astrofísica, Universidad Nacional Autónoma de México, Apdo. Postal 3-72, Morelia, Michoacán 58089, México*

²*CONACYT-Instituto Nacional de Astrofísica, Óptica y Electrónica, Luis E. Erro 1, 72840 Tonantzintla, Puebla, México*

Accepted 2021 December 9. Received 2021 December 7; in original form 2021 October 8

ABSTRACT

We investigate the effect of numerical magnetic diffusion in magnetohydrodynamic (MHD) simulations of magnetically supported molecular clouds. To this end, we have performed numerical studies on adaptive mesh isothermal simulations of marginally subcritical molecular clouds. We find that simulations with low and intermediate resolutions collapse, contrary to what is theoretically expected. However, the simulation with the highest numerical resolution oscillates around an equilibrium state without collapsing. In order to quantify the numerical diffusion of the magnetic field, we ran a second suit of current-sheet simulations in which the numerical magnetic diffusion coefficient can be directly measured and computed the corresponding diffusion times at various numerical resolutions. On this basis, we propose a criterion for the resolution of magnetic fields in MHD simulations based on requiring that the diffusion time to be larger than the characteristic time-scale of the physical process responsible for the dynamic evolution of the structure.

Key words: magnetic fields – MHD – methods: numerical – magnetic fields – ISM: clouds – ISM:magnetic fields.

1 INTRODUCTION

Magnetohydrodynamic simulations of the formation and evolution of molecular clouds have played an important role in the study of molecular clouds and star formation, either for the magnetic support model, where magnetic fields are responsible for supporting the clouds and their substructures against gravitational collapse (Shu et al. 1987; Mouschovias 1991), or for the turbulent support model, where the main support mechanism is the dynamical pressure generated by turbulence (Elmegreen 2000; Mac Low & Klessen 2004). Therefore, it is important to study the effects of numerical dissipation of the magnetic field on magnetohydrodynamic simulations of molecular clouds and their substructure.

One common way of measuring the importance of magnetic fields in the support of molecular clouds and their substructure is by computing the mass-to-flux ratio, denoted by μ when normalized to a critical value for marginal support, which depends on the geometry, but is otherwise a constant. When a cloud is magnetically supported against gravitational collapse, it is referred to as subcritical and, the-

oretically, $\mu < 1$. In this case, the cloud is expected to contract partially and then attain a hydrostatic configuration, flattened along the field direction (Mouschovias & Spitzer 1976). Otherwise, the cloud is said to be supercritical, undergoes gravitational collapse, and has $\mu > 1$ (Mestel & Spitzer 1956). However, if the magnetic field is insufficiently resolved, it is possible that a simulation which is in principle subcritical may nevertheless undergo spurious gravitational collapse due to numerical diffusion of the magnetic flux.

Resolution criteria are necessary for the adequate numerical simulation of every physical process. For example, Truelove et al. (1997) found that resolving the Jeans length with a minimum of four cells avoids spurious fragmentation on AMR hydrodynamic simulations of isothermal molecular clouds. Additionally, Bate & Burkert (1997) found a similar resolution condition for SPH simulations. Also, Koyama & Inutsuka (2004) found that at least three cells are necessary to resolve the Field length and to achieve convergence of some properties such as the number of clouds formed by thermal instability and the maximum Mach number in simulations of the development of turbulent motions driven by the non-linear evolution of thermal instability. More recently, Federrath et al. (2011) studied the gravity-turbulence-driven magnetic field amplification of supercrit-

* E-mail: g.granda@irya.unam.mx

† E-mail: e.vazquez@irya.unam.mx

‡ E-mail: g.gomez@irya.unam.mx

ical clouds. They found that it is necessary to resolve the Jeans length with at least 30 cells in order to resolve turbulence at the Jeans scale and capture minimum dynamo amplification of the magnetic field.

Resolution criteria are generally obtained by means of convergence tests, which consist of increasing the resolution until a certain feature of the flow remains invariant as the resolution is increased. In this sense, convergence tests constitute a trial-and-error procedure. In this work, we propose instead a resolution criterion based on measuring a “numerical diffusion coefficient” via a test problem, from which the dependence of the numerical diffusion time-scale on the resolution can be inferred and compared with the characteristic timescale of the physical process being investigated, thus providing a physically-motivated prescription for the necessary resolution. Specifically, the requirement is that the diffusion time needs to be longer than the relevant dynamical time of the structure. In this paper, we present an application to the problem of adequately resolving the magnetic support against the self-gravity of a dense molecular cloud core.

The paper is organized as follows. In section 2, we present a suite of numerical simulations of marginally magnetically subcritical molecular clouds at various resolutions, which undergo spurious collapse when the magnetic field is insufficiently resolved. In section 3, we propose a resolution criterion based on estimating the physical characteristic time-scale of the physical process being simulated, a measurement of the numerical diffusion coefficient by means of a test simulation, and apply it to the problem of magnetic cloud support. In section 4, the suite of simulations aimed at computing the numerical magnetic diffusion coefficient is presented. In section 5, we derive the numerical magnetic diffusion coefficient and apply our criterion to the magnetic cloud support simulations, finding an agreement with the resolution needed to resolve the support. In section 6, we discuss the implications of our results and present our conclusions.

2 MOLECULAR CLOUD SIMULATIONS

2.1 Numerical set-up

In this section, we present a suite of numerical simulations of magnetic support in molecular clouds using the adaptive mesh refinement (AMR) code FLASH, version 4.5, (Fryxell et al. 2000; Dubey et al. 2008; Dubey et al. 2009), and the ideal magnetohydrodynamic (MHD) multi-wave HLL-type solver (Waagan et al. 2011). The gravitational solver applied for these simulations is the OctTree algorithm also included in FLASH (Wünsch et al. 2018), while for the adaptive refinement, we use the Löhner’s error estimation applied to the density (Löhner 1987).

We consider an isothermal cloud that is marginally supported by the magnetic field (i.e. marginally subcritical), and find the minimum numerical resolution necessary for the cloud to actually be supported, rather than collapsing due to the loss of magnetic support caused by numerical diffusion. Each of these simulations has the same initial conditions and starts with an initial effective resolution of 32 cells per dimension, although each simulation reaches a different maximum resolution (see Table 1). They also include

periodic boundary conditions for both the magnetohydrodynamics and the self-gravity.

The initial conditions consist of an initially uniform magnetic field along the x -axis of $25.17 \mu\text{G}$, a box size of 10 pc, and a density perturbation of a 3D Gaussian profile on top of a background density ρ_0 :

$$\rho = \rho_0 \left\{ 1 + A \exp \left[- \frac{1}{2\sigma^2} (x^2 + y^2 + z^2) \right] \right\}, \quad (1)$$

where A and σ are constants which represent the perturbation amplitude and a measure of the perturbation size respectively. For this simulation, $\rho_0 = 2.12 \times 10^{-22} \text{ g cm}^{-3}$, $A = 1.50$, $\sigma = 2.5 \text{ pc}$. This set-up results in a total mass in the computational volume of $4.14 \times 10^3 M_\odot$, a Jeans’ length of 2.66 pc, given by

$$\lambda_J = \sqrt{\frac{\pi c_s^2}{G\rho}}, \quad (2)$$

where $c_s = 0.2 \text{ km s}^{-1}$ is the sound speed, and a mass-to-flux ratio $\mu = 0.53$ where we considered spherical geometry.

It is important to notice that this estimated value for the mass-to-flux ratio ($\mu = 0.53$) yields in practice a marginally subcritical molecular cloud because it does not include the contribution of the external gas and magnetic pressures on the computation of the critical mass-to-flux ratio (Shu 1992) and/or the flat geometry of the cloud due the mass accretion along the magnetic field lines (Strittmatter 1966). The marginal nature of the subcritical condition is an important feature, since otherwise the cloud evolution should not be very different for simulations with similar numerical resolutions.

2.2 Results of the simulations

As mentioned in the previous section, the three simulations have identical physical parameters and differ only in the maximum resolution allowed in each of them. We find that, while the low (MC7) and medium resolution (MC8) simulations undergo collapse after 9.6 and 9.8 Myr, respectively, a dense structure is formed and oscillates around an equilibrium state for the high-resolution run (MC9).

The evolution of the intermediate (MC8) and high-resolution (MC9) simulations are shown in Fig. 1.¹ Both simulations start their evolution in a very similar way (top left and top right panels), collecting gas on the central part of the computational domain along the magnetic field direction. The maximum density in both simulations increases and eventually reaches a plateau on its temporal evolution which is shown in Fig. 2. The time to reach the plateau density value is different in each simulation. We attribute this to the presence of different levels of numerical diffusion at each resolution, so that magnetic support is lost more rapidly at lower resolution. Therefore, we consider a different, but dynamically equivalent, time in each simulation, defined as the time at which the maximum density reaches the plateau stage on its temporal evolution. We call this stage the dynamically equivalent for the different simulations. The dynamically equivalent times are 7.8, 7.0, and 5.4 Myr for the

¹ This and the other plots present in this manuscript were done using yt project (Turk et al. 2011).

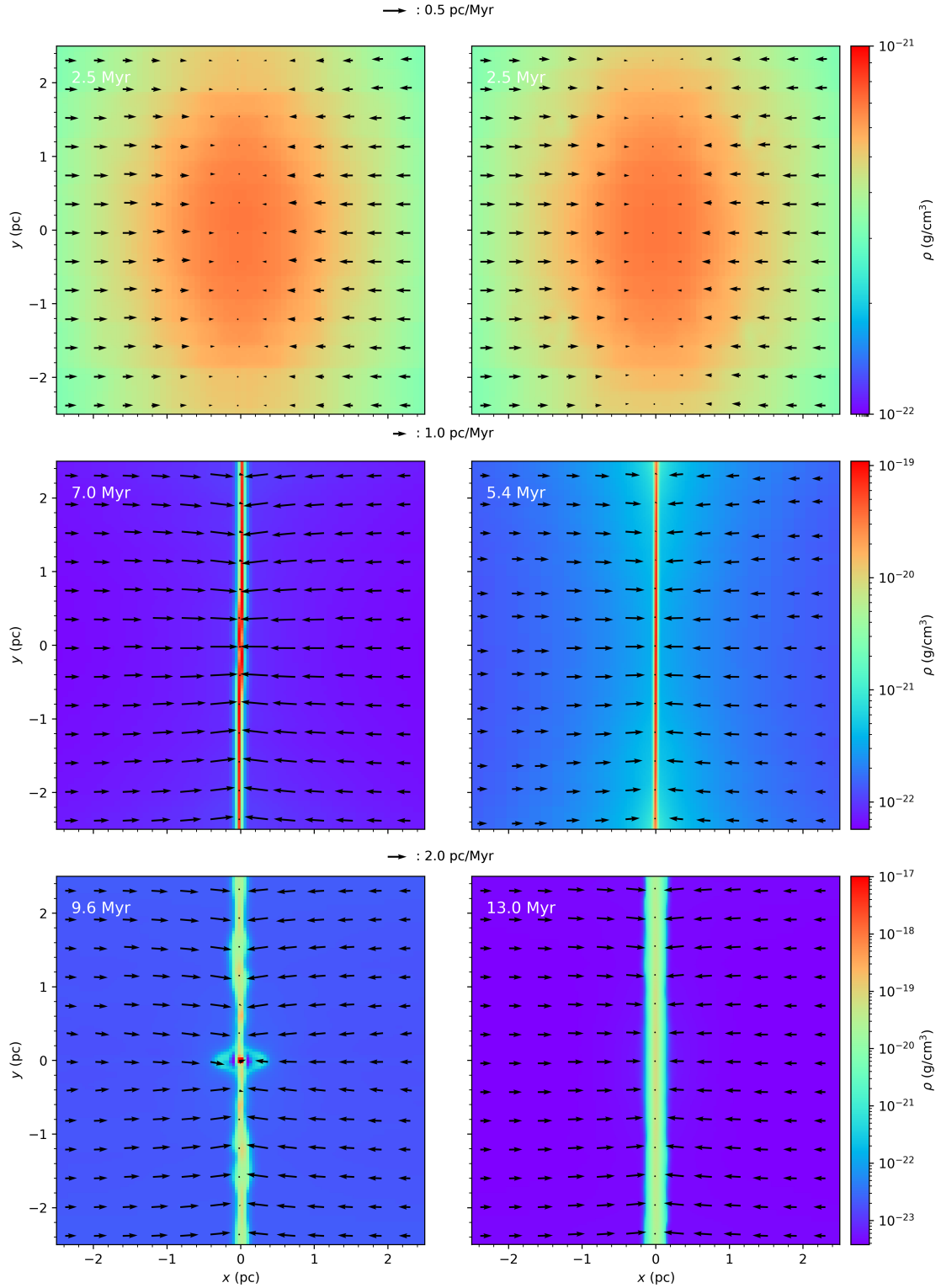


Figure 1. Zoomed cross section through the $z = 0$ plane. Colours represent gas density and the velocity field is represented by the black arrows. Left column correspond to the MC8 simulation while right column to the MC9 simulation. Note the different evolution times for each simulation. Simulation MC8 has already developed a collapsed object at its center by $t = 9.6$ Myr, while run MC9 has not done it even by $t = 13.0$ Myr.

Table 1. Molecular cloud simulations. In the first, second and third columns the simulation’s name, it’s effective and maximum resolution is shown. In the fourth column, we show the magnetic pressure gradient magnitudes computed at half the Jean’s length. The diffusion coefficients, free-fall times, diffusion times and collapse times at the dynamically equivalent time (see text) are shown in the fifth, sixth, seventh and eight columns respectively.

Simulation	Effective resolution	Maximun resolution (pc)	$ \nabla P_B $ (dyn/cm ³)	η (pc ² /Myr)	τ_{ff} (Myr)	τ_d (Myr)	τ_{coll} (Myr)
MC7	128	7.81×10^{-2}	1.565×10^{-29}	0.293	0.428	0.083	9.6
MC8	256	3.91×10^{-2}	1.041×10^{-29}	0.036	0.353	0.384	9.8
MC9	512	1.95×10^{-2}	1.218×10^{-30}	0.001	0.697	51.907	–

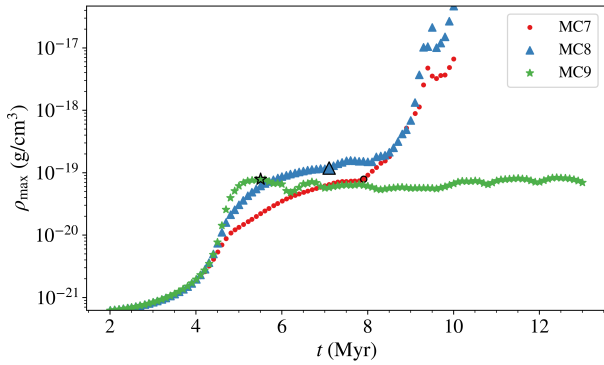


Figure 2. Temporal evolution of the maximum density in each of the MC simulations. The dark edge-colored \bullet , \blacktriangle , \star represent the dynamical equivalent densities for the MC7, MC8, and MC9 simulations respectively.

simulations MC7, MC8, and MC9 respectively, and we consider them as the computation snapshots for the diffusion and dynamical times estimates (see Section 5.3).

After the dynamically equivalent stage, the final evolution state of each simulation depends on whether the resolution was enough for solving the magnetic field correctly or not. For MC8, as shown in the bottom left panel of Fig. 1, the structure collapses due to the poor numerical resolution, or equivalently, to its high numerical magnetic diffusion coefficient. On the contrary, as shown in the bottom right panel of this figure, MC9 oscillates around an equilibrium state without collapsing in agreement with its subcritical condition. Therefore, numerical diffusion of the magnetic field can cause a spurious collapse of a marginally sub-critical molecular cloud.

3 RESOLUTION CRITERION

In the previous section, we empirically found the resolution necessary to properly resolve the magnetic support of a sub-critical molecular cloud. However, it would be desirable to have a more physically motivated, predictive criterion which can then be used in simulations in regard to effects other than the magnetic field. Since the evolution of any physical process is controlled by its relevant dynamical time, we propose a resolution criterion based on comparing the numerical diffusion time in a given simulation to the dynamical time of the physical process under investigation.

For subcritical molecular clouds, we obtain the relevant

dynamical times from the condition $\mu < 1$, which requires that the Alfvén crossing time be less than the free-fall time:

$$\tau_A < \tau_{ff}, \quad (3)$$

where the Alfvén crossing time is given by

$$\tau_A = L/v_A, \quad (4)$$

with L being the relevant spatial scale and v_A the Alfvén velocity. In turn, the free-fall time is given by

$$\tau_{ff} = \left(\frac{3\pi}{32G\rho} \right)^{1/2}, \quad (5)$$

where G is the gravitational constant. To obtain the resolution criterion, we compare the diffusion time with these time scales.

The diffusion time in the simulation may be obtained using the fact that the effect of the spatial discretization due to the numerical grid on the evolution of magnetic fields can be computed in terms of a magnetic diffusivity coefficient η (e.g. Bodenheimer 2007). Hence, a diffusion time may be computed in terms of η ,

$$\tau_d = L^2/\eta, \quad (6)$$

where η is the numerical magnetic diffusion coefficient. So, a smaller η means a larger diffusion time and ideal MHD is achieved when it is equal to zero.

When the numerical magnetic diffusion is large and controls the dynamics of the structure, we have

$$\tau_d < \tau_A. \quad (7)$$

In this case, the evolution of the structure is not physical because it is driven by numerical diffusivity and the Alfvén waves up to the wavelength for which $\tau_d = \tau_A$ are damped by numerical diffusion.

Increasing the numerical resolution reduces the numerical magnetic diffusion coefficient, so, the numerical magnetic diffusion time given by equation (6) increases. Therefore, the numerical resolution should be increased until the numerical diffusion and dynamical times fulfill the relation

$$\tau_{ff}, \tau_A < \tau_d. \quad (8)$$

When relation (8) is satisfied, the diffusion time is larger than the dynamical time of the mechanism responsible for the support of the molecular cloud, namely the propagation of MHD waves, for which the relevant time-scale is the Alfvén crossing time. Therefore, when relation (8) is satisfied, Alfvén waves can propagate without significant numerical diffusion during a free-fall time,² and thus our proposed

² Note that we will actually consider *twice* the free-fall time as

resolution criterion based on the characteristic time-scales of the problem consists in finding a numerical resolution which ensures that relation (8) is satisfied. The problem becomes now the estimation of the numerical diffusion time-scale as a function of resolution.

4 HARRIS-LIKE CURRENT-SHEET SIMULATIONS

In order to apply the resolution criterion given by relation (8), we first need to measure the numerical magnetic diffusion coefficient η . With this in mind, we simulate a Harris-like current-sheet (e.g. Skála et al. 2015; Kliem et al. 2000). This simulation consists in setting up a magnetic field configuration that reverses direction across a narrow region, maintaining total (thermal + magnetic) pressure equilibrium. Following the set-up of Skála et al. (2015), these simulations are two dimensional and isothermal with a computational domain of $[-5, 5]$ pc on the x -axis, $[-0.6, 0.6]$ pc on the y -axis, and open and periodic boundary conditions in the x and y directions, respectively. Note that these simulations do not include self-gravity.

The initial density and magnetic field intensity are given by

$$\rho = (P_{\text{tot}} - P_{B,\text{par}} \tanh^2(x)) / c_s^2, \quad (9)$$

$$B_y = (8\pi P_{B,\text{par}})^{1/2} \tanh(x), \quad (10)$$

where $P_{\text{tot}} = P_{\text{th}} + P_B$ is the total pressure, $P_{\text{th}} = c_s^2 \rho$ is the thermal pressure, and $P_B = B^2/8\pi$ is the magnetic pressure. $P_{B,\text{par}}$ is the asymptotic value of the magnetic pressure at large x .

Numerical magnetic diffusion disrupts the initial pressure equilibrium in the central region of the computational domain, which is the region where the gradient of the magnetic field is the largest. In order to measure the magnetic diffusion coefficient on this region, we consider the induction equation in the presence of resistivity:

$$\frac{\partial \mathbf{B}}{\partial t} + \nabla \times (\mathbf{B} \times \mathbf{v}) = -\nabla \times (\eta \nabla \times \mathbf{B}), \quad (11)$$

where \mathbf{v} is the fluid velocity, which, for our pressure equilibrium configuration, is zero. Assuming that η is uniform in space, we obtain

$$\eta = \frac{\left(\frac{\partial B}{\partial t}\right)}{\left(\frac{\partial^2 B}{\partial x^2}\right)}. \quad (12)$$

Hence, in order to measure the numerical resistivity corresponding to a given resolution, we performed the suite of simulations described in Table 2, in which the derivatives appearing in eq. (12) are to be measured. Each of the simulations has the same initial conditions but different numerical resolution. The simulations were performed with the same version of the FLASH code and MHD solver.

the relevant time-scale because numerical simulations consistently show this to be the order of the actual collapse time, since the thermal pressure gradient is not negligible during the first stages of the collapse (e.g., Larson 1969; Galván-Madrid et al. 2007; Naranjo-Romero et al. 2015).

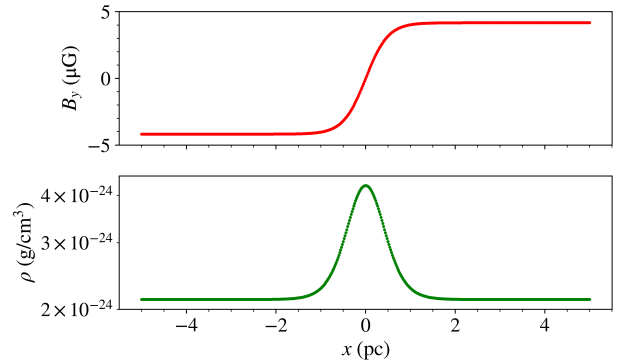


Figure 3. Magnetic field and density initial conditions for the Harris-like simulations.

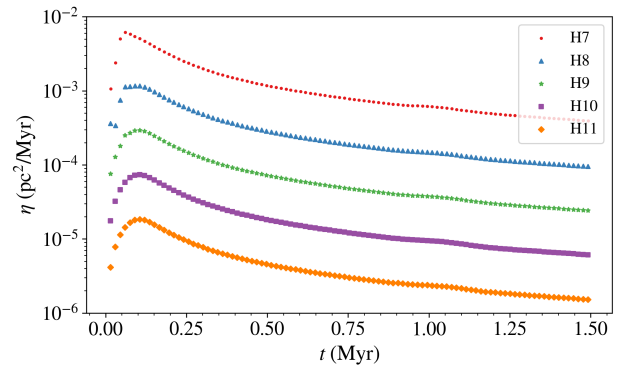


Figure 4. η versus time for the Harris-like simulations.

5 RESULTS

5.1 Numerical magnetic diffusion coefficients of the Harris-like simulations

To measure the numerical magnetic diffusion coefficients of each of the simulations presented in Table 2, where we have set the initial conditions to obtain the density and magnetic field profiles shown in Fig. 3. We evaluated numerically equation (12) on the point $(x_m, y_m) = (-0.5493 \text{ pc}, 0) \equiv (-x_0, 0)$, which is the point where the magnetic field strength is half of its maximum magnitude. The magnetic diffusion coefficient measured over time, following the prescription by Skála et al. (2015), is shown in Fig. 4. As expected, a higher resolution yields a smaller numerical magnetic diffusion coefficient, thus a larger diffusion time.

Since η varies in time, we consider its maximum value at each resolution as the measured value to avoid that the time term present on the denominator of the discretization of equation (12) dominates its temporal evolution. The resulting numerical diffusion coefficients are listed in the third column of Table 2.³

³ We also computed the diffusion parameters for the eight-wave MHD solver included in the FLASH 4.5 distribution. These results are shown in Appendix A

Table 2. Harris-like simulations. The first and second columns represent the simulation name and its resolution respectively. The third and fourth columns represent numerical magnetic diffusion coefficients and magnetic pressure gradient magnitudes.

Simulation	Resolution (pc)	η (pc ² /Myr)	$ \nabla P_B $ (dyn/cm ³)
H7	7.81×10^{-2}	6.164×10^{-3}	3.289×10^{-31}
H8	3.91×10^{-2}	1.170×10^{-3}	3.406×10^{-31}
H9	1.95×10^{-2}	2.950×10^{-4}	3.393×10^{-31}
H10	9.75×10^{-3}	7.399×10^{-5}	3.383×10^{-31}
H11	4.88×10^{-3}	1.849×10^{-5}	3.377×10^{-31}

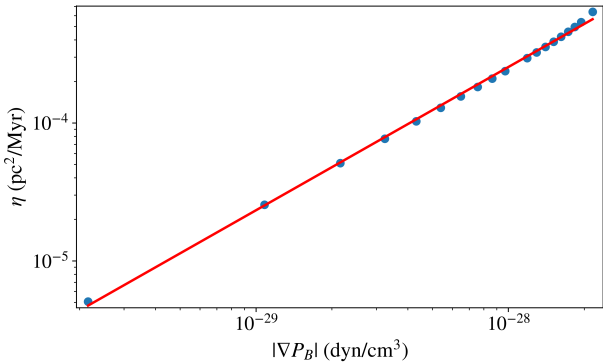


Figure 5. The numerical diffusivity η versus the magnetic pressure gradient magnitude. The blue points represent the measured values while the red line is a fit to those points.

5.2 Scaling of η for different conditions

In addition to depending on the resolution, the value of the numerical magnetic diffusion coefficient depends also on the magnetic field derivatives in the region where it is measured. In order to estimate this dependence, we performed several Harris-like current sheet simulations for a range of values of the magnetic pressure parameter $P_{B,\text{par}}$ (see eq. 10) while keeping the same numerical resolution and the same width of the central transition region (i.e., keeping the same value of x_0) used in simulation H7. Thus, varying $P_{B,\text{par}}$ is equivalent to varying the magnetic pressure gradient, since x_0 is kept constant.

For this set of simulations, we chose values of $P_{B,\text{par}}$ that correspond to magnetic field values in the range of [10.56, 105.64] μG . We find that η scales almost linearly with the magnetic pressure gradient, as shown in Fig. 5, for which we obtained a fit given by $\log(\eta) \approx 25.48 + 1.04 \log(|\nabla P_B|)$. We attribute this behavior to the fact that, in the Harris simulations, the driver of the numerical diffusion is the magnetic pressure gradient. Therefore, this result allows us to incorporate different values of the magnetic field gradient into the computed value for η by making the correction

$$\eta_2 = \eta_1 \frac{|\nabla P_{B2}|}{|\nabla P_{B1}|}, \quad (13)$$

where η_2 and η_1 are the numerical magnetic diffusion coefficient under the conditions of magnetic pressure gradient ∇P_{B2} and ∇P_{B1} respectively. In our case, this allows us to

use the derived values for η in the Harris-like simulations. We, therefore, proceed as follows: For a given refinement level, the pressure gradient, ∇P_{B1} , is measured at the same point as η_1 (see section 5.1) in the Harris-like simulations. These measurements are listed in the third column of Table 2. In the molecular cloud simulations, ∇P_{B2} is measured at a distance equal to half the Jeans length from the cloud's center, since we are studying the evolution of a molecular cloud that would collapse in the absence of magnetic support, therefore, the Jeans length is the relevant characteristic length scale. Therefore, using the measured values for η_1 , $|\nabla P_{B1}|$, $|\nabla P_{B2}|$ (listed in Tables 2 and 1), as well as equation (13), we obtain the values of η_2 also listed in Table 1). In turn, this allows us to compute the diffusion time and compare it with the free-fall time to ensure that the numerical resolution is enough to correctly model the dynamical evolution.

5.3 Diffusion and dynamical times

According to eq. (6), the diffusion time-scales can be obtained from the numerical magnetic diffusion coefficients and the spatial scale across which the magnetic field is being diffused. As mentioned in the previous subsection, we consider half the Jeans length as the diffusion length scale. The diffusion and free-fall times are computed at the time when the simulations reach their dynamically equivalent state (see Section 2) are listed in Table 1. It is worth noting that the computed free-fall times differ only slightly for the different resolution simulations, while the estimated diffusion times vary by almost 3 orders of magnitude, as a consequence of the strong dependence of the magnetic diffusion coefficient on numerical resolution. Specifically, for the MC7 and MC8 simulations, the diffusion time is smaller than twice the free-fall time. In other words, the numerical diffusion of the magnetic field controls the dynamics of these clouds. Unsurprisingly, the subcritical cloud spuriously collapses.

In contrast, for the MC9 simulation, the diffusion time is larger than twice the free-fall time. So, this simulation is not dominated by the numerical diffusion of the magnetic field and it does not collapse.

In conclusion, the results from this section show that our resolution criterion, based on comparing the numerical diffusion time scale with the characteristic time-scale of the physical problem, is consistent with the resolution empirically found to be necessary in order to correctly simulate the magnetic support of a cloud in Section 2.

6 DISCUSSION AND CONCLUSIONS

In this work, we have found that a numerical simulation of a marginally magnetically subcritical molecular cloud undergoes spurious collapse if the numerical resolution is insufficient, and presented two different approaches to estimate the resolution required in order to properly resolve the magnetic support. The first one consisted in a study of the evolution of a marginally sub-critical molecular cloud, finding that when the resolution is poor, numerical diffusion of the magnetic field causes the spurious collapse of the cloud. The second approach consisted in the implementation of a physically motivated resolution criterion, relying on the comparison of

the numerical magnetic diffusion time implied by the resolution used with the relevant dynamical time, in this case, (twice) the free-fall time.

This criterion recovers the required resolution, but in addition, it provides a physical interpretation and a *predictive* procedure for the choice of the required resolution, provided some additional numerical tests are performed in order to estimate the numerical diffusion for a given physical process, using a given solver. For example, for cold atomic clumps that can grow from thermal instabilities in the presence of a magnetic field on time-scales of the order of the cooling time, we may compare this dynamical timescale with the magnetic diffusion time and obtain equations analogous to (7) and (8).

It is important to note that, in this work, we have restricted our study to the effect of numerical magnetic diffusion on the evolution and collapse of subcritical molecular clouds. On the other hand, in the case of supercritical clouds with $\mu > 1$, the relation between the free-fall and the Alfvénic crossing times corresponding to that presented in equation (3) becomes instead

$$\tau_{\text{ff}} < \tau_{\text{A}}. \quad (14)$$

In this case, collapse always occurs but, if the resolution is insufficient, the collapse may occur too rapidly, since it is known that the magnetic forces can in principle delay it (e.g., Ostriker et al. 1999). Thus, the required numerical resolution to avoid this situation is the one that ensures the fulfillment of

$$\tau_{\text{ff}} < \tau_{\text{A}} < \tau_{\text{d}}. \quad (15)$$

Therefore, insufficient resolution in either the subcritical or supercritical cases may lead to an overestimation of the star formation rate.

ACKNOWLEDGEMENTS

This research was supported by a CONACYT scholarship. We are thankful to Adriana Gazol and José Juan González Avilés for their helpful comments and feedback, to Robi Banerjee for providing the MHD solver, and to the referee, James Beattie, for useful comments.

DATA AVAILABILITY

The data underlying this article will be shared on reasonable request to the corresponding author.

REFERENCES

- Bate M. R., Burkert A., 1997, *Monthly Notices of the Royal Astronomical Society*, 288, 1060
- Bodenheimer P., ed. 2007, *Numerical Methods in Astrophysics: An Introduction*. Series in Astronomy and Astrophysics, Taylor & Francis, New York
- Dubey A., Reid L. B., Fisher R., 2008, *Physica Scripta Volume T*, 132, 014046
- Dubey A., Antypas K., Ganapathy M. K., Reid L. B., Riley K., Sheeler D., Siegel A., Weide K., 2009, *Parallel Computing*, 35, 512
- Elmegreen B. G., 2000, *The Astrophysical Journal*, 530, 277

- Federrath C., Sur S., Schleicher D. R. G., Banerjee R., Klessen R. S., 2011, *The Astrophysical Journal*, 731, 62
- Fryxell B., et al., 2000, *The Astrophysical Journal Supplement Series*, 131, 273
- Galván-Madrid R., Vázquez-Semadeni E., Kim J., Ballesteros-Paredes J., 2007, *The Astrophysical Journal*, 670, 480
- Kliem B., Karlicky M., Benz A. O., 2000, *Astronomy & Astrophysics*, 360, 715
- Koyama H., Inutsuka S.-i., 2004, *The Astrophysical Journal*, 602, L25
- Larson R. B., 1969, *Monthly Notices of the Royal Astronomical Society*, 145, 271
- Lohner R., 1987, *Computer Methods in Applied Mechanics and Engineering*, 61, 323
- Mac Low M.-M., Klessen R. S., 2004, *Reviews of Modern Physics*, 76, 125
- Mestel L., Spitzer Jr. L., 1956, *Monthly Notices of the Royal Astronomical Society*, 116, 503
- Mouschovias T. C., 1991, in *NATO Advanced Science Institutes (ASI) Series C*. p. 61
- Mouschovias T. C., Spitzer Jr. L., 1976, *The Astrophysical Journal*, 210, 326
- Naranjo-Romero R., Vázquez-Semadeni E., Loughnane R. M., 2015, *The Astrophysical Journal*, 814, 48
- Ostriker E. C., Gammie C. F., Stone J. M., 1999, *The Astrophysical Journal*, 513, 259
- Shu F. H., 1992, *The Physics of Astrophysics. Volume II, Volume II*, University Science Books, Sausalito, Calif.
- Shu F. H., Lizano S., Adams F. C., 1987, in *Star Forming Regions*. pp 417–433
- Skála J., Baruffa F., Büchner J., Rampp M., 2015, *Astronomy & Astrophysics*, 580, A48
- Strittmatter P. A., 1966, *Monthly Notices of the Royal Astronomical Society*, 132, 359
- Truelove J. K., Klein R. I., McKee C. F., Holliman II J. H., Howell L. H., Greenough J. A., 1997, *The Astrophysical Journal Letters*, 489, L179
- Turk M. J., Smith B. D., Oishi J. S., Skory S., Skillman S. W., Abel T., Norman M. L., 2011, *ApJS*, 192, 9
- Waagan K., Federrath C., Klingenberg C., 2011, *Journal of Computational Physics*, 230, 3331
- Wünsch R., Walch S., Dinnbier F., Whitworth A., 2018, *MNRAS*, 475, 3393

APPENDIX A: MAGNETIC DIFFUSION COEFFICIENTS FOR THE EIGHT-WAVE FLASH MHD SOLVER

The magnetic diffusion coefficients and magnetic pressure gradients obtained for the standard FLASH MHD solver eight-wave are shown in Table A1.

These values were computed with the same procedure and initial conditions described in Section 4. The scaling of η for different conditions was also performed in the way described in Section 5.2, obtaining $\log(\eta) \approx 25.49 + 1.04 \log(|\nabla P_B|)$.

This paper has been typeset from a $\text{\TeX}/\text{\LaTeX}$ file prepared by the author.

Table A1. Magnetic diffusion for the 8-wave MHD solver. The first and second columns represent the simulation name and its resolution respectively. The third and fourth columns represent numerical magnetic diffusion coefficients and magnetic pressure gradient magnitudes.

Simulation	Resolution (pc)	η (pc ² /Myr)	$ \nabla P_B $ (dyn/cm ³)
H7	7.81×10^{-2}	4.209×10^{-3}	3.289×10^{-31}
H8	3.91×10^{-2}	1.040×10^{-3}	3.400×10^{-31}
H9	1.95×10^{-2}	2.772×10^{-4}	3.389×10^{-31}
H10	9.75×10^{-3}	7.179×10^{-5}	3.378×10^{-31}
H11	4.88×10^{-3}	1.819×10^{-5}	3.371×10^{-31}